Origin of the Attraction in Aliphatic C−H/π Interactions: Infrared Spectroscopic and Theoretical Characterization of Gas-Phase Clusters of Aromatics with Methane

So-ichi Morita,[†] Asuka Fujii,*[,†] Naohiko Mikami,[†] and Seiji Tsuzuki*[,‡]

Department of Chemistry, Graduate School of Science, Tohoku University, Sendai 980-8578, Japan, and National Institute of Advanced Industrial Science and Technology (AIST), Tsukuba, Ibaraki 305-8568, Japan

Received: July 8, 2006; In Final Form: July 14, 2006

An attractive intermolecular interaction between an aliphatic C−H bond and a π-electron system (C−H/π interaction) was characterized on the basis of infrared spectroscopy and high level ab initio calculations. Infrared spectroscopy was applied to several isolated methane clusters with benzene, toluene, *p*-xylene, mesitylene, and naphthalene in the gas phase, and the spectral changes of the C−H stretch bands in the methane moiety upon the cluster formation were observed. In the theoretical approach, interaction energies of the clusters were evaluated by high-level ab initio calculations. The forbidden symmetric C−H stretch transition weakly appeared in the IR spectra of the clusters, and it confirmed the small deformation of the methane moiety from the T_d symmetry, which was predicted by the ab initio calculations. On the other hand, the degenerated asymmetric C−H stretch band showed complicated splitting, which is qualitatively interpreted by a hindered rotor model. Low-frequency shifts upon the cluster formation were seen in the symmetric C−H stretch frequency, though the magnitude of the shifts was extremely small and no clear correlation with the interaction energy was found. On the other hand, the size of the calculated interaction energy well correlates with the polarizability of aromatics. The S_1-S_0 electronic transition of the aromatic moiety was also observed, and it showed low-frequency shifts upon cluster formation. These results support the dominance of the dispersion interaction over the electrostatic and charge-transfer terms in the aliphatic C−H/π interaction.

Introduction

Understanding of weak intermolecular interactions is one of the important keys to elucidate mechanisms of complicated molecular functions in macromolecules.[1] The C−H/π interaction is a weak attractive interaction between a C−H bond and a π electron system, and it has been a subject of much interest as a crucial driving force in determining crystal packing, molecular conformation, and alignment of liquid crystal.[1−3]

The nature of the C−H/π interaction has been a controversial issue.[1,2] Though it has been claimed repeatedly that the C−H/π interaction is a hydrogen bond,[4−8] it has not yet been clearly confirmed whether the magnitude and orientation dependence of the C−H/π interaction are similar to those of the conventional hydrogen bond or not. The acidity of a C−H bond is generally much weaker than those of O−H and N−H bonds; therefore, the C−H/π interactions are believed to lie in the critical region between the weak hydrogen bond and the van der Waals interaction.[1,9,10] The acidity of a C−H bond actually shows strong dependence on its hybridization type; while the acidity of a C−H bond of alkane is extremely low (pK_a=59 in methane), remarkable enhancement of the acidity is seen in alkenes and alkynes (pK_a=45 and 25 in ethylene and acetylene, respectively).[11] Electron-withdrawing halo-substituents also enhance the acidity (pK_a=24 in chloroform).[12] Therefore, it is expected that the nature of the C−H/π interaction changes from the dominance of the dispersion force (van der Waals type interaction) to enhanced contribution of the electrostatic force (π-hydrogen bond like interaction) with an increase of the acidity of the C−H bond.

The π-hydrogen bond-like nature of the C−H/π interaction of acetylene has been pointed out by theoretical calculations and spectroscopic signatures,[4,9,13−16] and it is often called "activated" C−H/π interaction.[2] The interaction between chloroform and aromatics is another type of the "activated" CH/π interaction, and it also has large electrostatic contributions.[17] On the other hand, the nature of the "typical" (not activated) C−H/π interactions between aliphatic C−H bonds and π-electron systems, such as that in benzene−methane, is still controversial in nature. Most of the C−H bonds in nature are "typical" C−H bonds, and "activated" C−H bonds are rather exceptional. Therefore understanding the nature of the "typical" C−H/π interaction is necessary. Theoretical calculations of the ethylene−methane cluster in the early stage insisted that the major source of attraction was electrostatic and charge-transfer interactions.[18] However, recent high-level ab initio calculations of the benzene−methane cluster and other C−H/π clusters show the dominance of the dispersion force.[8,10,14,17,19−26] The estimated interaction energy of the benzene−methane cluster agrees well with the recently reported experimental interaction energy in the gas phase,[10] and it demonstrates the high reliability of the calculations. The dominance of the dispersion force indicates that the "typical" C−H/π interaction should be distinguished from a π-hydrogen bond, where the electrostatic interaction is the major source of attraction. With respect to this point, observation of the aliphatic C−H stretching vibration in aromatics−methane clusters is strongly required as the frequency shift upon cluster formation is a remarkable marker to judge the nature of the C−H/π interaction. Unfortunately, however, no measurement of definite frequency shifts of the aliphatic

* Corresponding authors e-mail: asukafujii@mail.tains.tohoku.ac.jp (A.F.) and s.tsuzuki@aist.go.jp (S.T.)
† Tohoku University.
‡ AIST.

10.1021/jp064297k CCC: $33.50
Published on Web 08/22/2006

C−H stretching vibrations associated with the "typical" C−H/π interaction has been reported.

In the present study, we probe the nature of the "typical" C−H/π interaction by infrared (IR) spectroscopy of substituted benzene−methane clusters in a supersonic jet in combination with high level ab initio calculations. We measured the IR spectra of the C−H stretching vibrations of the methane moiety in X−methane clusters (X=benzene, toluene, *p*-xylene, mesitylene (1,3,5-trimethylbenzene), and naphthalene). Characterization of the nature of the C−H/π interaction was carried out on the basis of the spectral changes upon the cluster formation. With the substitution and change of the aromatic ring number, electronic properties of the aromatic moiety such as multiple moments and polarizability were varied. Correlation between the spectral changes and variation of the electronic properties of the aromatic moiety was examined. The interaction energies of the clusters were evaluated by high-level ab initio calculations. The calculated interaction energies were compared with the size of frequency shifts and with the polarizabilities of the aromatics to reveal the origin of the attraction in the clusters. The magnitude of electrostatic and dispersion interactions in the C−H/π interaction was also discussed.[27]

Experiments

Infrared spectra of the X−methane clusters in the C−H stretching vibrational region were measured by infrared-ultraviolet (IR−UV) double resonance spectroscopy.[9] Details of the apparatus were described in elsewhere,[9,10] and only a brief description is given here.

Clusters in a molecular beam are irradiated by a pulsed UV laser, of which the wavelength is fixed at the S_1-S_0 transition of the cluster. The mass-selected ion signal due to the multiphoton ionization via the S_1 vibronic level of the cluster is monitored as a measure of the population of the cluster in the ground state. A pulsed IR laser is introduced prior to the UV laser pulse by 50 ns, and the wavelength of the IR light is scanned over the C−H stretch region. When the IR wavelength is resonant on the vibrational transition of the cluster, the decrease of the vibrational ground-state population of the cluster due to the IR absorption is detected as the decrease of the ion signal. Thus, by scanning the IR wavelength while monitoring the ion signal, the IR spectrum of the cluster is measured as a depletion spectrum.

Aromatic samples were purchased from Aldrich Co. and were used without further purification. The vapor of the aromatic sample is seeded in a neon/methane gaseous mixture of the stagnation pressure at 2−4 atm. The methane concentration is adjusted to be 15−20%, and the vapor pressure of the aromatic sample is controlled by the sample reservoir temperature for the optimization of the cluster signal intensity. The gaseous mixture is expanded into a vacuum chamber through a pulsed valve with an orifice of 0.8 mm diameter. The supersonic expansion is skimmed by a skimmer, and the resultant molecular beam is introduced into the interaction region of a Wiley−McLaren type mass spectrometer. Ions produced by the multiphoton ionization are mass-selected by the mass spectrometer and are detected by a channel electron multiplier.

Theoretical Calculations

The Gaussian 03 programs were used for the ab initio molecular orbital calculations.[28] Dunning's correlation consistent basis sets (cc-pVDZ, aug-cc-pVDZ, and aug-cc-pVTZ)[29,30] and a modified 6-311G** basis set were used. The aug(d,p)-6-311G** basis set is a 6-311G** basis set augmented with diffuse d functions ($\alpha_d(C) = 0.1565$ on carbon atoms and diffuse p functions ($\alpha_p(H) = 0.1875$) on hydrogen atoms).[31] Electron correlation was accounted for by the second-order Mϕller−Plesset perturbation (MP2) method[32,33] and by coupled cluster calculations with single and double substitutions with noniterative triple excitations [CCSD(T)].[34] The basis set superposition error (BSSE) was corrected for all calculations by using the counterpoise method.[35,36]

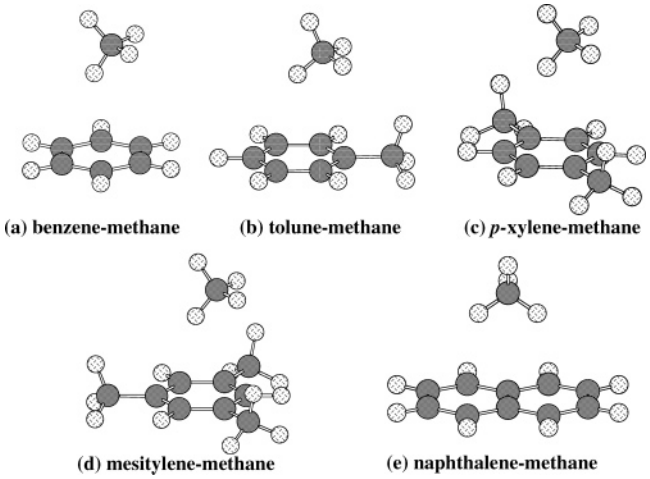

Figure 1. Optimized structures of X−methane clusters at the MP2/aug(d,p)-6-311G** level.

The geometries of clusters were optimized at the MP2/aug-(d,p)-6-311G** level. Vibrational frequencies were calculated at the same level. The MP2 level interaction energy at the basis set limit [$E_{MP2(limit)}$] was estimated by the method of Helgaker et al.[37] from the calculated MP2 interaction energies using the aug-cc-pVDZ and aug-cc-pVTZ basis sets. In the method of Helgaker et al., the calculated MP2 interaction energies with the Dunning's correlation consistent basis sets were fitted to the form $a + bX^{-3}$ (where X is 2 for aug-cc-pVDZ, 3 for aug-cc-pVTZ). The $E_{MP2(limit)}$ was then estimated by extrapolation. The method of Helgaker et al. was originally proposed for the estimation of electron correlation contribution at the basis set limit. But we have used this method for the estimation of $E_{MP2(limit)}$, as the basis set dependence of the HF interaction energy is negligible. The CCSD(T) level interaction energy at the basis set limit [$E_{CCSD(T)(limit)}$] was estimated as the sum of the estimated $E_{MP2(limit)}$ and CCSD(T) correction term (the difference between the calculated CCSD(T) and MP2 level interaction energies using cc-pVDZ basis set).[14] The electrostatic energies of the clusters were calculated with ORIENT version 3.2.[38] The electrostatic energy was obtained from the interactions between distributed multipoles of monomers.[39,40] Distributed multipoles up to hexadecapole on all atoms were obtained from the MP2/6-311G** wave functions of isolated monomers using the CADPAC version 6.[41]

Results and Discussion

1. Optimized Structures of X−Methane Clusters. Optimized structures of X−methane clusters (X=(**a**) benzene, (**b**) toluene, (**c**) *p*-xylene, (**d**) mesitylene, and (**e**) naphthalene) are shown in Figure 1. The optimized structures show that the methane prefers to locate above the benzene ring in the benzene and substituted benzene clusters (**a**−**d**), and a single C−H bond points to the ring plane, as is expected from the C−H/π interaction. On the other hand, the methane is placed on the border of the two ring units in the naphthalene cluster (**e**). The optimized naphthalene cluster has the C_s symmetry. The angles

TABLE 1: Calculated Interaction Energies in X−Methane Clusters (X=Benzene, Toluene, *p*-Xylene, Mesitylene, and Naphthalene)[a]

	MP2/cc-pVDZ	MP2/aug-cc-pVDZ	MP2/aug-cc-pVTZ	$E_{MP2(limit)}$[b]	CCSD(T)/cc-pVDZ	ΔCCSD(T)[c]	$E_{CCSD(T)(limit)}$[d]	D_0[e]
$C_6H_6-CH_4$	−0.649	−1.528	−1.742	−1.831	−0.333	0.316	−1.515	1.174
$C_6H_5Me-CH_4$	−0.795	−1.872	−2.111	−2.211	−0.420	0.375	−1.836	1.349
$C_6H_4Me_2-CH_4$	−0.883	−1.922	−2.155	−2.254	−0.498	0.386	−1.868	1.472
$C_6H_3Me_3-CH_4$	−1.008	−2.136	−2.383	−2.487	−0.582	0.426	−2.061	1.664
$C_{10}H_8-CH_4$	−1.107	−2.500	−2.781	−2.898	−0.500	0.607	−2.292	1.753

[a] Interaction energy in kcal/mol. The MP2/aug(d,p)-6-311G** level optimized geometries of the clusters (Figure 1) were used. [b] Estimated MP2 level interaction energy at the basis set limit by the method of Helgaker et al. [c] CCSD(T) correction term. The difference between the calculated CCSD(T) and MP2 level interaction energies using the cc-pVDZ basis set. [d] Estimated CCSD(T) level interaction energy at the basis set limit. The sum of $E_{MP2(limit)}$ and ΔCCSD(T). $E_{CCSD(T)(limit)}$ corresponds to $-D_e$. [e] Binding energy including vibrational zero-point energy (ZPE). $D_0 = D_e - \Delta ZPE$ (ΔZPE is the change of ZPEs by the formation of cluster).

TABLE 2: Electrostatic and Dispersion Energies of X−Methane Clusters (X=Benzene, Toluene, *p*-Xylene, Mesitylene, and Naphthalene)[a]

	E_{HF}[b]	E_{total}[c]	E_{es}[d]	E_{rep}[e]	E_{corr}[f]
$C_6H_6-CH_4$	1.16	−1.52	−0.08	1.24	−2.67
$C_6H_5Me-CH_4$	1.46	−1.84	0.06	1.40	−3.30
$C_6H_4Me_2-CH_4$	1.40	−1.87	−0.02	1.42	−3.27
$C_6H_3Me_3-CH_4$	1.55	−2.06	0.02	1.54	−3.62
$C_{10}H_8-CH_4$	1.90	−2.29	−0.08	1.97	−4.19

[a] Energy in kcal/mol. [b] HF level interaction energy calculated using the aug-cc-pVTZ basis set. [c] Estimated CCSD(T) interaction energy at the basis set limit. [d] Electrostatic energy. See text. [e] Repulsion energy ($= E_{HF} - E_{es}$). See text. [f] Correlation interaction energy ($= E_{total} - E_{HF}$). See text.

between the interacting C−H bond and the aromatic plane in the clusters (**a**−**e**) are 60°, 42°, 55°, 52°, and 28°, respectively.

The interaction energies of the clusters were calculated using the optimized structures, as listed in Table 1. In the previous paper, we have examined the quantitative reliability of ab initio calculations to evaluate the C−H/π interaction by the direct comparison between the experimentally and theoretically determined interaction energies of the benzene−methane cluster.[10] We have found that a large basis set near saturation is necessary for quantitative evaluation of the interaction energy and that the MP2 calculations overestimate the attraction compared with the more reliable CCSD(T) calculations. The estimated CCSD(T) level interaction energy at the basis set limit [$E_{CCSD(T)(limit)}$] of the cluster agrees well with the experimental binding energy after zero-point vibrational energy correction.[10]

The polarizability of methane (2.593×10^{-24} cm^3) is nearly the same as that of krypton (2.484×10^{-24} cm^3).[42] The size of calculated interaction energies [$E_{CCSD(T)(limit)}$] of the methane clusters are close to that of the krypton cluster with benzene ($D_0 < 1.15$ kcal/mol), which is a typical van der Waals cluster.[43] The nearly same size of interaction energy suggests the dominance of the dispersion interaction term in the C−H/π interaction of the methane clusters.

The electrostatic energies (E_{es}) of the clusters are summarized in Table 2. E_{total} is the estimated $E_{CCSD(T)(limit)}$. E_{corr} is the effect of electron correlation on the calculated total interaction energy, which is the difference between E_{total} and E_{HF} (HF level interaction energy using the aug-cc-pVTZ basis set). The dispersion interaction is the major contributor to E_{corr}. E_{rep} ($= E_{HF} - E_{es}$) is mainly exchange-repulsion energy, but it also includes some other terms.

The E_{es} is almost negligible in all the clusters (less than 0.1 kcal/mol). Due to the small contribution of electrostatic term, the Hartree−Fock level interaction energy (E_{HF}) is always repulsive. The large E_{corr} values show that dispersion is the major source of attraction in the clusters.

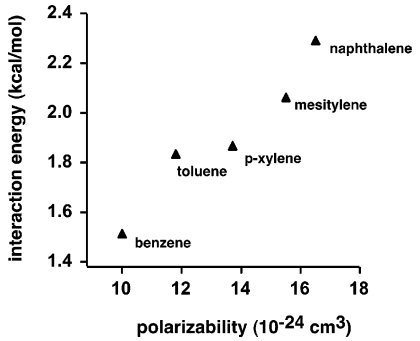

Figure 2. Plot of the polarizability of the aromatic moiety (monomer molecule) versus $E_{CCSD(T)(limit)}$ of the cluster. The polarizability values are taken from ref 42.

With an increase of the methyl substitution, the total interaction energy of the clusters increases as shown in Table 1. Our calculations show that the contribution of electrostatic interaction to the attraction is very small as shown in Table 2, which indicates that the increase of the electron density of the benzene ring by the electron donating methyl groups is not the primary cause of the enhancement of the attraction by the methyl substituents. The calculated interaction energies [$E_{CCSD(T)(limit)}$] have a clear correlation with experimental polarizabilities of the aromatic moiety as seen in Figure 2, which shows that the dispersion interaction is the major source of the attraction in the clusters.

Although the interacting C−H bond is not perpendicular to the benzene plane in the optimized structures (**a**−**d**), the magnitude of the calculated tilt angle in the optimized cluster geometry is not important. The potential energy surfaces of the clusters are very shallow with respect to the rotation of methane. For example, the interaction energy of the optimized structure (**a**) in Figure 1, where the C−H bond is tilted, calculated at the MP2/aug(d,p)-6-311G** level (−1.58 kcal/mol) is very close to that of the optimized structure imposing the C_{3v} symmetry restriction (−1.56 kcal/mol) (Figure 3). The very small energy difference (0.02 kcal/mol) shows that the C−H bond can change its tilt angle very easily in the cluster. The calculated tilt angle may largely change associated with a very small change of the interaction energy by the choice of the calculation level. The very weak orientation dependence of the interaction energy suggests that the hydrogen atom is not essential to the attraction. The large contribution of dispersion for the attraction also supports the idea, as most of the dispersion interaction comes from that between carbon atoms and the contribution of the hydrogen atom is much less.

The methane does not locate above the center of a benzene ring in the naphthalene−methane cluster (**e**). The benzene−methane cluster-like structure is not a local minimum. Our

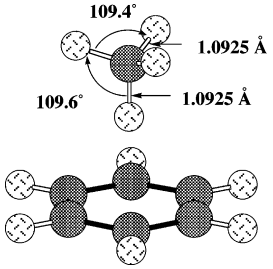

Figure 3. Optimized structure of the benzene−methane cluster at the MP2/aug(d,p)-6-311G** level with imposing the C_{3v} symmetry restriction.

TABLE 3: Vibronic Band Positions of the Observed Clusters

	S_1-S_0 vibronic band	transition frequency (cm^{-1})[a]
benzene−CH_4	6^1_0	38567 (−39)
toluene−CH_4	0^0_0	37432 (−43)
p-xylene−CH_4	0^0_0	36677 (−56)
mesitylene−CH_4	6^1_0	36974 (−27)
naphthalene-−CH_4	$\bar{8}^1_0$	32444 (−11)

[a] Values in parentheses are frequency shifts from the corresponding monomer bands.

calculations show that dispersion is the major source of attraction in the cluster, which suggests that the methane locates above the border of the two benzene rings (Figure 1(**e**)) to maximize the dispersion interaction.

2. Electronic Spectroscopy. In IR−UV double resonance spectroscopy, a S_1-S_0 vibronic transition of the cluster is used to monitor the ground-state population transfer due to the IR absorption. Table 3 summarizes the S_1-S_0 vibronic band positions of the X−methane clusters used to measure the present study. All the transitions are localized in the aromatic moiety of the clusters. In benzene and mesitylene, the origin band of the S_1-S_0 transition is symmetry forbidden, and the 6^1_0 vibronic band was used to monitor the ground-state population. Though the origin band of naphthalene is an allowed transition, its transition intensity is very weak. Then, the strong $\bar{8}^1_0$ band was used to monitor. The electronic transition of the benzene−methane cluster was first reported by Schauer and Bernstein,[44] and other cluster bands are reported for the first time, to our knowledge.

All the electronic transitions of the X−methane clusters show low-frequency shifts upon the cluster formation. In aromatic clusters of the van der Waals type, such as benzene-rare gas clusters, the S_1-S_0 electronic transition localized in the aromatic moiety is generally low-frequency shifted,[45] while a high-frequency shift is generally seen in π-hydrogen-bonded clusters such as benzene−water.[46] Benzene−acetylene and benzene−chloroform are known to show the high-frequency shifts in the S_1-S_0 transition,[9,47−49] and it reflects the π-hydrogen-bond nature of their intermolecular interactions. The low-frequency shifts of the X−methane clusters are in contrast with the trend of these "activated" C−H/π interaction type clusters, suggesting the major contribution of the dispersion force in the X−methane clusters. It is also worth noting that the magnitude of the low-frequency shift of the electronic transition is very different in each cluster, and no systematic trend is seen. The frequency shift of the electronic transition arises from the stabilization energy difference between the S_0 and S_1 states. Different stabilization energies in the S_1 state would be responsible to the very different frequency shifts because the electronic character is more remarkably perturbed by substitution effects and vibronic coupling in the S_1 state than in the S_0 state.

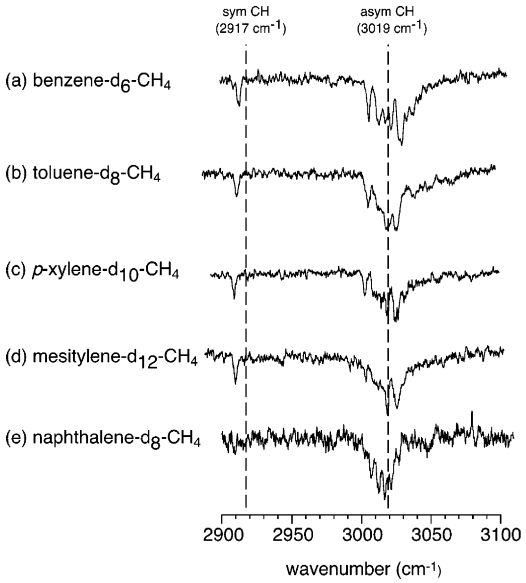

Figure 4. IR spectra of X−methane clusters in the C−H stretching vibrational region (X=(a) benzene-d_6, (b) toluene-d_8, (c) *p*-xylene-d_{10}, (d) mesitylene-d_{12}, and (e) naphthalene-d_8). The IR−UV double resonance spectroscopy technique was used to measure the IR spectra of the clusters. All the observed bands are due to the vibrations of the methane moiety of the clusters.

3. Infrared Spectroscopy. Figure 4 shows the IR spectra of the X−methane clusters (X=(a) benzene-d_6, (b) toluene-d_8, (c) *p*-xylene-d_{10}, (d) mesitylene-d_{12}, and (e) naphthalene-d_8) in the C−H stretching vibrational region. To avoid the spectral interference due to the C−H stretches of the aromatic moiety, all-deuterated aromatic samples were used to measure these IR spectra. Thus, all the observed bands in the spectra are due to the C−H stretch bands of the methane moiety of the clusters. These IR spectra correspond to the IR absorption spectra of the clusters in the vibrational ground level of the S_0 state.

Bare methane is of the T_d symmetry group, and it has two C−H stretching vibrational modes. The ν_1 mode is an IR inactive symmetric C−H stretch mode (a_1), and its fundamental frequency has been determined to be 2917 cm^{-1} by Raman spectroscopy.[50] The other C−H stretch mode is the triply degenerated ν_3 mode (t_2). This is an IR active mode, and its frequency is reported to be 3019 cm^{-1}.[50] In comparison with the vibrations in bare methane, the observed bands in the X−methane clusters are easily assigned. A weak single band around 2910 cm^{-1} is attributed to the symmetric C−H stretch, and the complicated manifold around 3020 cm^{-1} is assigned to the asymmetric C−H stretches of the methane moiety.

Figure 5 shows the expansion of the IR spectra of the X−methane clusters in the symmetric C−H stretch region. The symmetric C−H stretch band is symmetry-forbidden in the bare molecule, and its appearance in the clusters demonstrates that the symmetry of the methane moiety is lowered from T_d to C_{3v} (or lower), where the a_1 symmetry vibration is IR active. The vibrational frequency of the ν_1 band of the clusters shows the very small low-frequency shifts of 5−8 cm^{-1} in comparison with that of bare methane. This indicates the elongation of the C−H bonds of the methane moiety due to the C−H/π interaction, though the very small frequency shifts reflect the very small magnitude of the elongation.

Such deformation of the methane moiety in the clusters is also confirmed in the optimized structures. Table 4 shows the calculated C−H bond distances and the ν_1 frequencies of the methane moiety. The C−H bond distances of the methane

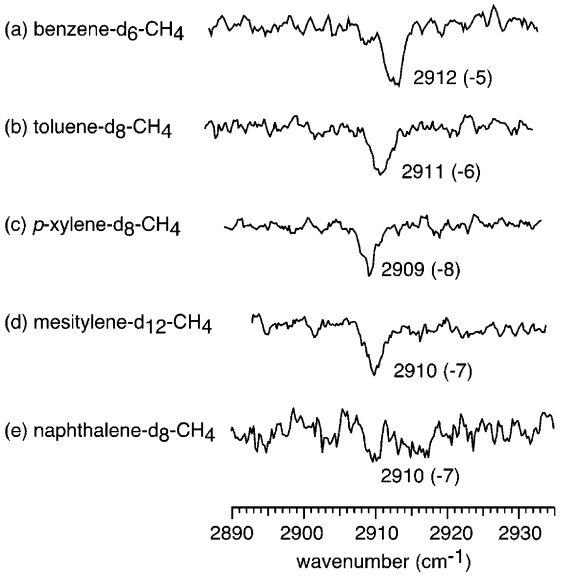

Figure 5. Expanded IR spectra of the X−methane clusters (X=(a) benzene-d_6, (b) toluene-d_8, (c) *p*-xylene-d_{10}, (d) mesitylene-d_{12}, and (e) naphthalene-d_8) in the symmetric C−H stretch band of the methane moiety. Values in parentheses are the frequency shifts from that of bare methane (2917 cm^{-1}).

TABLE 4: Calculated C−H Bond Distance and Symmetric C−H Stretching (ν_1) Vibrational Frequencies of the Methane Moiety in the X−Methane Clusters[a]

	C−H bond distance (Å)		
	interacting C−H	free C−H	ν_1 frequency (cm^{-1})[b]
bare CH_4		1.0919	3058 (0)
benzene−CH_4	1.0925	1.0926, 1.0924	3053 (−5)
toluene−CH_4	1.0926	1.0927	3050 (−8)
p-xylene−CH_4	1.0927	1.0928, 1.0925	3050 (−8)
mesitylene−CH_4	1.0928	1.0928	3049 (−9)
naphthalene−CH_4	1.0933	1.0927, 1.0930	3046 (−12)

[a] Geometry optimization and vibrational frequency analysis were carried out at the MP2/aug(d,p)-6-311G** level. No scaling factor is applied to the vibrational frequencies. [b] Values in parentheses are frequency shifts from that of bare CH_4.

moiety in the clusters are 0.0005−0.0011 Å longer than that of bare methane, and this is much smaller than the magnitude of the typical elongation of the O−H bond in hydrogen bond formation (0.01−0.1 Å).[51] In the table, the C−H bond facing the aromatic ring is called "interacting", and other C−H bonds are called "free". The calculated bond distances of "interacting" C−H bonds are not largely different from "free" C−H bonds. In addition, Figure 3 shows that the change of H−C−H bond angles upon cluster formation is mainly responsible for the lowering of symmetry. These are indications that the C−H/π interaction is not localized in the "interacting" C−H bonds, but the interaction slightly deforms the whole methane moiety.

A low-frequency shift of a X−H stretch band is a well-known marker of hydrogen bond formation, though previous ab initio calculations on benzene−methane have predicted a high-frequency shift of the ν_1 mode (+15 cm^{-1}) and shortening of the C−H bonds (−0.0008 Å) of the methane moiety.[52] As summarized in Table 4, however, the present calculations predicted the low-frequency shifts and C−H bond distance elongation, which are consistent with the observed IR spectra.[53] The calculated frequency shifts reproduced the observed magnitude of the shifts. This proves the reliability of the calculated C−H bond distance elongation.

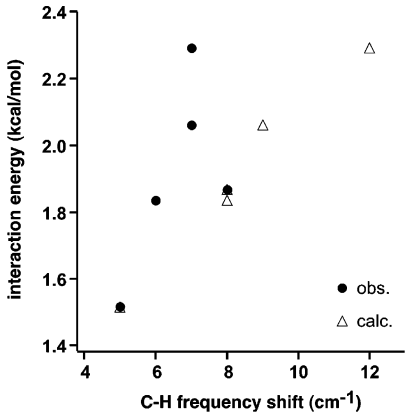

Figure 6. Plot of the observed (closed circle) and calculated (open triangle) frequency shifts of the ν_1 (symmetric C−H stretch) mode of the methane moiety versus the calculated interaction energy in the X−methane clusters.

Figure 6 shows plots of the observed and calculated frequency shifts of the ν_1 mode of the methane moiety versus the calculated interaction energy in the X−methane clusters. The magnitude of the observed C−H frequency shifts is extremely small, and correlation between the observed shift and the interaction energy ($E_{CCSD(T)(limit)}$) is not clear. This is in contrast with typical hydrogen-bonded systems, where the magnitude of the O(N)−H stretch frequency shift well correlates to the interaction strength.[51] The calculated shifts show rather better correlation to the interaction energy, but the agreement with the observed shifts becomes poor with an increase of the interaction energy. The magnitude of the shifts is so small that the theoretical evaluation of the shifts seems to be difficult.

The contribution of the charge transfer has been a controversial issue on the C−H/π interaction.[18] The C−H frequency shift is a good marker also to the contribution of the charge transfer because the charge transfer in the hydrogen bond, i.e., the electron density transfer from the proton accepting site to the σ^* orbital of the X−H bond, should cause the low-frequency shift of the X−H bond. Though the low-frequency shifts of the C−H stretch band are consistent with the contribution of the charge transfer to the C−H/π interaction, the magnitude of the observed shifts is extremely small. In the case of the "activated" C−H/π interaction, for example, the C−H stretch of the acetylene site in benzene−acetylene shows the low-frequency shift of 22 cm^{-1}.[9,16] Moreover, typical low-frequency shifts of the O−H stretch in ordinary hydrogen-bonded systems are of 100−400 cm^{-1}.[51] The extremely smaller magnitude of the frequency shifts in the X−methane clusters supports the previous suggestion by the high level ab initio calculations that the contribution of the charge transfer is not essential in the C−H/π interaction.[8,10,14,17,19−26] As theoretical evaluation of the contribution of the charge transfer, we calculated the charge distributions in the X−methane clusters. The atomic charge distributions of the clusters were obtained by Mulliken population analysis and by electrostatic potential fitting with the Merz−Singh−Kollman scheme[55,56] from the calculated MP2 wave functions of the clusters to evaluate the amount of charge transfer from aromatics to methane. The calculated total charge of the methane moiety is summarized in Figure 7. Though the weak basis-set dependence is seen, all the calculations clearly demonstrate that the total charge in the methane moiety is very small (<0.015 au), and the magnitude of the charge transfer is almost negligible.

The asymmetric C−H stretch band of the X−methane clusters shows complicated band structures in the IR spectra, as seen in

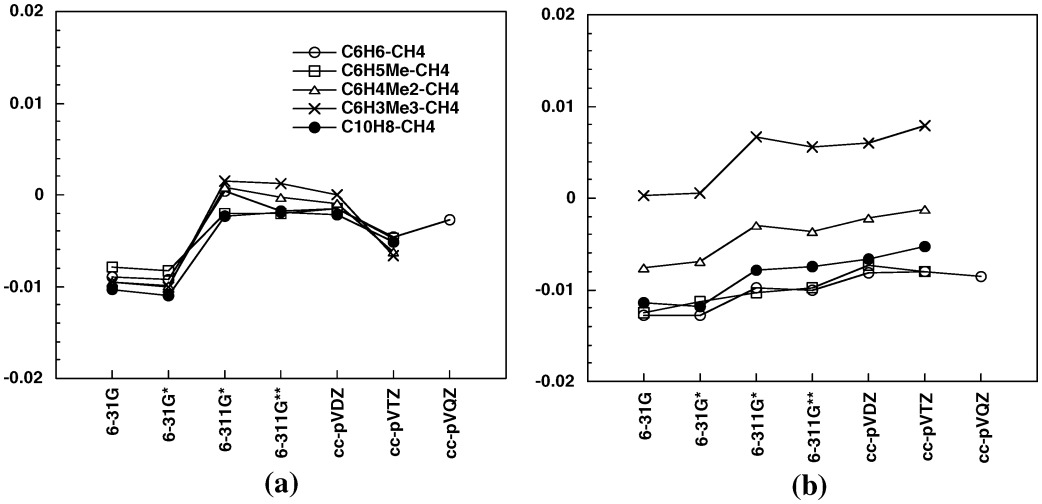

Figure 7. Calculated total charge in the methane moiety of X−methane clusters obtained from the MP2 level wave functions: (a) atomic charges were obtained by Mulliken population analysis and (b) atomic charges were obtained by electrostatic potential fitting.

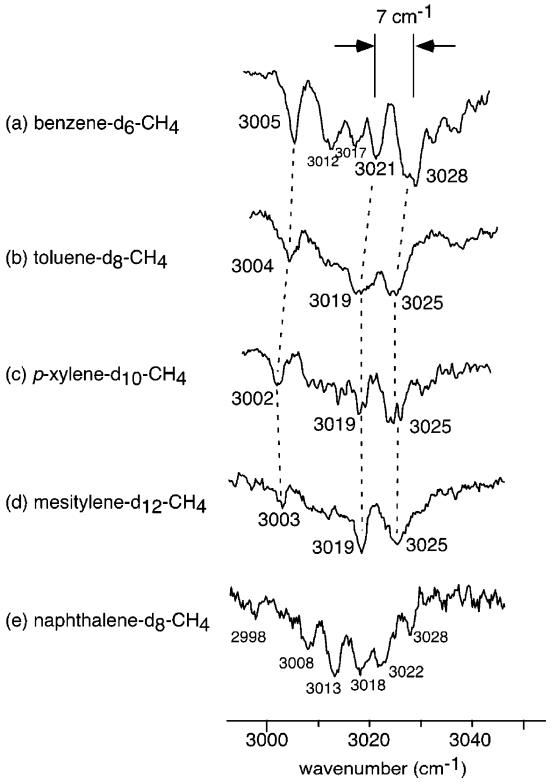

Figure 8. Expanded IR spectra of X−methane ((X=(a) benzene-d_6, (b) toluene-d_8, (c) *p*-xylene-d_{10}, (d) mesitylene-d_{12}, and (e) naphthalene-d_8) in the asymmetric C−H stretch region of the methane moiety.

the expanded spectra in Figure 8. The asymmetric C−H stretching vibration in bare methane is a triply degenerated mode (t_2), and lowering of the symmetry due to the cluster formation would lift this degeneracy. In addition to the three major bands, however, a few more bands are seen in the manifold. Therefore, the internal rotation of the methane moiety should be responsible for the complicated band structure. If the methane moiety is freely rotating on the aromatic ring plane, the effective symmetry of the methane moiety should be T_d, and the symmetric C−H stretch band should disappear. Therefore, the appearance of the symmetric C−H stretch band indicates that the C−H bond is bound to the aromatic ring plane even though this directionality of the C−H bond is not essential for the magnitude of the interaction energy. In contrast to the asymmetric C−H stretch band, the symmetric stretch band seems to show no sign of the internal rotation. Such a difference between the rotational structures is qualitatively interpreted by a simple model of hindered rotation of the methane moiety.[57,58]

Our previous high level ab initio calculations demonstrated that the C_{3v} on-top structure, which is schematically shown in Figure 3, is the most stable structure for benzene−methane.[10] Our calculations suggest that the H−C−H bond angle deformation lowers the symmetry of the methane moiety from T_d to C_{3v}. Then, the symmetric C−H stretching vibrational mode (a_1 in T_d) becomes IR active (a_1 in C_{3v}), and the asymmetric C−H stretching vibration (t_2 in T_d) splits into two IR-active modes of a_1 and e. When we suppose the hindered rotation of the C_{3v} methane moiety around the principal axis of the benzene moiety, as schematically shown in Figure 9, the rotational energy is expressed by

$$E = Bm^2$$

in which B is the rotational constant and $m = 0, \pm1, \pm2, ...$ The rotational levels of $|m| = 0, \pm1$, and ±2 are denoted as Σ, Π, and Δ, respectively.[57,58] When the transition dipole moment of the vibrational transition is parallel to the rotational axis, the selection rule for the rotational transition associated with the vibrational transition is $\Delta m = 0$. Then, all the rotational lines are overlapped like a Q branch, and the vibrational transition shows a single peak. On the other hand, for the vibrational transition by the transition dipole moment perpendicular to the rotational axis, the rotational selection rule is $\Delta m = \pm1$. The transition energy of the rotational part is $\Delta E = B(2m+1)$. Thus, the rotational structure due to the Π-Σ and Δ-Π rotational lines appears with the interval of $\Delta(\Delta E) = 2B$. The a_1 vibrations in C_{3v} have the transition dipole moment parallel to the rotational (principal) axis, and this is consistent with the single peak of the symmetric C−H stretch band. The transition dipole moments for the e vibrations are perpendicular to the rotational axis, and several rotational lines would appear with the interval of 2B. In the band manifold of the asymmetric C−H stretch, the lowest energy band at 3003−3005 cm^{-1} is attributed to the a_1 component, and the other two major bands at 3019−3021 and 3025−3028 cm^{-1} are assigned to the Π-Σ and Δ-Π rotational lines of the e component, respectively. These assignments based on the hindered rotor model are schematically summarized in Figure 9.

The observed interval of the Π-Σ and Δ-Π rotational lines is 7 cm^{-1} in benzene−methane and 6 cm^{-1} in toluene−methane,

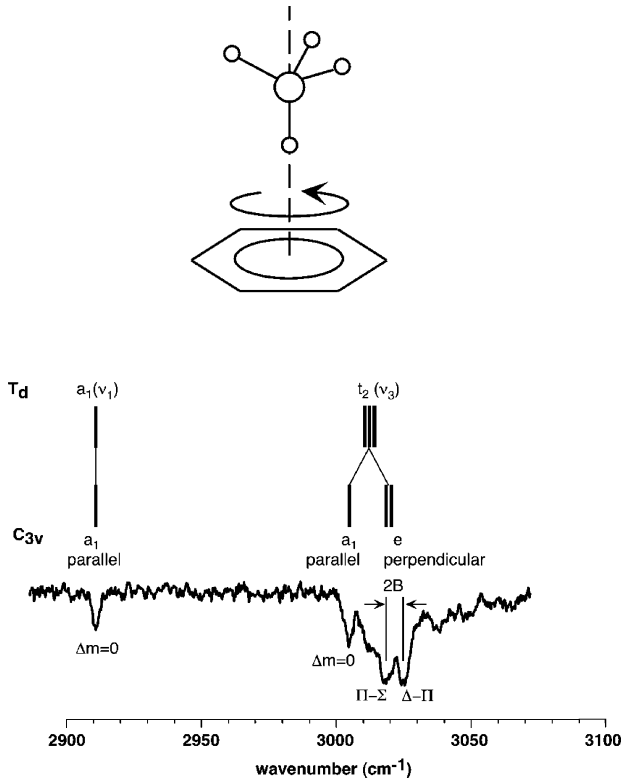

Figure 9. Schematic representation of the hindered rotor model (upper). Assignments for the C−H stretch band structures observed in toluene-d_8−methane on the basis of the hindered rotor model (see text) (lower).

p-xylene−methane, and mesitylene−methane. This means that the rotational constant of the hindered rotation is 3−3.5 cm^{-1} in these clusters. The rotational constant of bare methane is 5.24 cm^{-1},[57] and the small reduction of the rotational constant reflects the friction of the rotation. In benzene−methane, a few other bands are seen in the spectrum, and it suggests the coupling between the rotation and the torsional motions of the methane moiety.[58] With the introduction of the methyl substitution, the spectral feature converges into the three major bands, and other bands are suppressed. This spectral change would reflect that the internal rotation of the methyl group becomes more hindered with an increase in the number of the substituted group, and the hindered rotor model becomes a better approximation. In naphthalene−methane, on the other hand, the heavily dense band manifold is seen in the IR spectrum, and it is difficult to assign the bands by the simple hindered rotor model. As was shown in Figure 1(**e**), two C−H bonds of the methane moiety interact with the aromatic ring in naphthalene−methane, and even the rotation along the molecular axis perpendicular to the phenyl ring plane cannot be free. The more complicated potential barrier for the methane rotation may be responsible for the heavily dense manifold in naphthalene−methane.

Summary

The C−H/π interaction in the aromatics−methane clusters was characterized by IR spectroscopy of the C−H stretching vibrations of the methane moiety in combination with the high level ab initio calculations. The weak appearance and low-frequency shifts of the symmetric C−H stretch band in the IR spectra of X−methane demonstrated the small deformation of the methane moiety due to the cluster formation. No clear correlation was found between the observed C−H frequency shift and the interaction energy. Negligible contribution of the charge transfer was also supported by the small C−H frequency shifts in the IR spectra and by the calculated charge distribution. The calculated interaction energy of the cluster showed a clear correlation with the polarizability of the aromatic moiety, reflecting the dominant contribution of the dispersion interaction to the total interaction energy. Electrostatic interactions in the clusters were very small. Observed shifts of S_1-S_0 electronic transition of the clusters also suggest that the clusters are of the van der Waals type. These results indicate that aliphatic C−H/π interaction should be distinguished from hydrogen bond-like interactions. The nature of aliphatic "typical" C−H/π interaction is significantly different from that of the conventional hydrogen bond. The asymmetric C−H stretch bands in the IR spectra showed a complicated band structure, and the hindered rotor model gave the qualitative assignment of the band structure.

Acknowledgment. This work was partially supported by the MEXT Japan through projects (No. 1600200 and 17310057) of the Grant-in-Aid. The authors are grateful for help from Dr. Mitsuhiko Miyazaki in the early stage of this study. We thank Tsukuba Advanced Computing Center for the provision of the computational facilities. This work was also partly supported by the NAREGI Nanoscience Project, Ministry of Education, Culture, Sports, Science and Technology.

References and Notes

(1) Desiraju, G. R.; Steiner, T. *The Weak Hydrogen Bond*; Oxford University Press: New York, 1999.
(2) Nishio, M.; Hirota, M.; Umezawa, Y. *The CH/π interaction*; Wiley-VCH: New York, 1998; and references therein.
(3) Yamakawa, M.; Yamada, I.; Noyori, R. *Angew. Chem., Int. Ed.* **2001**, *40*, 2818.
(4) Philip, D.; Robinson, J. M. A. *J. Chem. Soc., Perkin Trans. 2* **1988**, 1643.
(5) Ehama, R.; Tsushima, M.; Yuzuri, T.; Suezawa, H.; Sakakibara, K. M.; Hirota, M. *Bull. Chem. Soc. Jpn.* **1993**, *66*, 814.
(6) Novoa, J. J.; Mota, F. *Chem. Phys. Lett.* **2000**, *318*, 345.
(7) Takahashi, O.; Kohno, Y.; Iwasaki, S.; Saito, K.; Iwaoka, M.; Tomoda, S.; Umezawa, Y.; Tsuboyama, S.; Nishio, M. *Bull. Chem. Soc. Jpn*. **2001**, *74*, 2421.
(8) Takahashi, O.; Kohno, Y.; Saito, K. *Chem. Phys. Lett*. **2003**, *378*, 509.
(9) Fujii, A.; Morita, S.; Miyazaki, M.; Ebata, T.; Mikami, N. *J. Phys. Chem. A* **2004**, *108*, 2652.
(10) Shibasaki, K.; Fujii, A.; Mikami, N.; Tsuzuki, S. *J. Phys. Chem. A* **2006**, *110*, 4397.
(11) Jones, M., Jr. *Organic Chemistry*, 2nd ed.; W. W. Norton & Company: New York, 2000.
(12) *Handbook of Chemistry*, 5th ed.; The Chemical Society of Japan Ed.; Maruzen Co.: Tokyo, 2004.
(13) Brand, J. C. D.; Eglinton, G.; Tyrrell, J. *J. Chem. Soc*. **1965**, 5914.
(14) Tsuzuki, S.; Honda, K.; Uchimaru, T.; Mikami, M.; Tanabe, K. *J. Am. Chem. Soc.* **2000**, *122*, 3746.
(15) Sundararajan, K.; Viswanathan, K. S.; Kulkarmi, A. D.; Gadre, S. R. *J. Mol. Struct.* **2002**, *613*, 209.
(16) Ramos, C.; Winter, P. R.; Stearns, J. A.; Zwier, T. S. *J. Phys. Chem. A* **2003**, *107*, 10280.
(17) Tsuzuki, S.; Honda, K.; Uchimaru, T.; Mikami, M.; Tanabe, K. *J. Phys. Chem. A* **2002**, *106*, 4423.
(18) Takagi, T.; Tanaka, A.; Matsuo, S.; Maezaki, H.; Tani, M.; Fujiwara, H.; Sasaki, Y. *J. Chem. Soc., Perkin Trans. 2* **1987**, 1015.
(19) Sakaki, S.; Kato, K.; Miyazaki, T.; Musashi, Y.; Ohkubo, K.; Ihara, H.; Hirayama, C. *J. Chem. Soc., Faraday Trans.* **1993**, *89*, 659.
(20) Tarakeshwar, P.; Choi, H. S.; Kim, K. S. *J. Am. Chem. Soc*. **2001**, *123*, 3323.
(21) Ribas, J.; Cubero, E.; Luque, F. J.; Orozco, M. J. *J. Org. Chem*. **2002**, *67*, 7057.
(22) Tsuzuki, S.; Honda, K.; Uchimaru, T.; Mikami, M.; Tanabe, K. *J. Phys. Chem. A* **1999**, *103*, 8265.
(23) Oki, M.; Takano, S.; Toyota, S. *Bull. Chem. Soc. Jpn*. **2000**, *73*, 2221.
(24) Sundararajan, K.; Sankaran, K.; Viswanathan, K. S.; Kulkarni, A. D.; Gadre, S. R. *J. Phys. Chem. A* **2002**, *106*, 1504.
(25) Sundararajan, K.; Viswanathan, K. S.; Kulkarni, A. D.; Gadre, S. R. *J. Mol. Struct.* **2002**, *613*, 209.

(26) Re, S.; Nagase, S. *J. Chem. Soc., Chem. Commun.* **2004**, 658.

(27) Several descriptors have been customarily used to discuss whether an interaction is a hydrogen bond or not. Geometrical and topological descriptors may be useful for judging whether an interaction can be called a hydrogen bond or not. But our aim is to reveal the nature (magnitude and orientation dependence) of the aliphatic C−H/π interaction to confirm whether the C−H/π interaction is important for the structures of molecular assemblies as for the hydrogen bond. The geometrical and topological descriptors are not so useful for this purpose. The comparison of the dispersion and electrostatic energies is essential to answer this question. The hydrogen bond is important for the structures of molecular assemblies, as the hydrogen bond is sufficiently strong and sufficiently directional (ref 1). The large electrostatic contribution to the attraction is the cause of these characteristic features of the hydrogen bond.

(28) *Gaussian 03, Revision C.02*; Frisch, M. J.; Trucks, G. W.; Schlegel, H. B.; Scuseria, G. E.; Robb, M. A.; Cheeseman, J. R.; Montgomery, J. A., Jr.; Vreven, T.; Kudin, K. N.; Burant, J. C.; Millam, J. M.; Iyengar, S. S.; Tomasi, J.; Barone, V.; Mennucci, B.; Cossi, M.; Scalmani, G.; Rega, N.; Petersson, G. A.; Nakatsuji, H.; Hada, M.; Ehara, M.; Toyota, K.; Fukuda, R.; Hasegawa, J.; Ishida, M.; Nakajima, T.; Honda, Y.; Kitao, O.; Nakai, H.; Klene, M.; Li, X.; Knox, J. E.; Hratchian, H. P.; Cross, J. B.; Bakken, V.; Adamo, C.; Jaramillo, J.; Gomperts, R.; Stratmann, R. E.; Yazyev, O.; Austin, A. J.; Cammi, R.; Pomelli, C.; Ochterski, J. W.; Ayala, P. Y.; Morokuma, K.; Voth, G. A.; Salvador, P.; Dannenberg, J. J.; Zakrzewski, V. G.; Dapprich, S.; Daniels, A. D.; Strain, M. C.; Farkas, O.; Malick, D. K.; Rabuck, A. D.; Raghavachari, K.; Foresman, J. B.; Ortiz, J. V.; Cui, Q.; Baboul, A. G.; Clifford, S.; Cioslowski, J.; Stefanov, B. B.; Liu, G.; Liashenko, A.; Piskorz, P.; Komaromi, I.; Martin, R. L.; Fox, D. J.; Keith, T.; Al-Laham, M. A.; Peng, C. Y.; Nanayakkara, A.; Challacombe, M.; Gill, P. M. W.; Johnson, B.; Chen, W.; Wong, M. W.; Gonzalez, C.; and Pople, J. A. Gaussian, Inc.: Wallingford, CT, 2004.

(29) Dunning, T. H., Jr. *J. Chem. Phys.* **1989**, *90*, 1007.

(30) Woon, D. E.; Dunning, T. H., Jr. *J. Chem. Phys.* **1993**, *98*, 1358.

(31) Tsuzuki, S.; Uchimaru, T.; Mikami, M.; Tanabe, K. *J. Phys. Chem. A* **1998**, *102*, 2091.

(32) Mφller, C.; Plesset, M. S. *Phys. Rev.* **1934**, *46*, 618.

(33) Head-Gordon, M.; Pople, J. A.; Frisch, M. J. *Chem. Phys. Lett.* **1988**, *153*, 503.

(34) Pople, J. A.; Head-Gordon, M.; Raghavachari, K. *J. Chem. Phys.* **1987**, *87*, 5968.

(35) Ransil, B. J. *J. Chem. Phys.* **1961**, *34*, 2109.

(36) Boys, S. F.; Bernardi, F. *Mol. Phys.* **1970**, *19*, 553.

(37) Helgaker, T.; Klopper, W.; Koch, H.; Noga, J. *J. Chem. Phys.* **1997**, *106*, 9639.

(38) Stone, A. J.; Dullweber, A.; Hodges, M. P.; Popelier, P. L. A.; Wales, D. J. *Orient: a program for studying interactions between molecules version 3.2*; University of Cambridge: 1995.

(39) Stone, A. J. *The theory of intermolecular forces*; Clarendon Press: Oxford, 1996.

(40) Stone, A. J.; Alderton, M. *Mol. Phys.* **1985**, *56*, 1047.

(41) Amos, R. D. *CADPAC*: *The Cambridge Analytical Derivatives Package, Issue 6*; Technical report; University of Cambridge: 1995. A suite of quantum chemistry programs developed by Amos, R. D. with contributions from Alberts, I. L.; Andrews, J. S.; Colwell, S. M.; Handy, N. C.; Jayatilaka, D.; Knowles, P. J.; Kobayashi, R.; Laidig, K. E.; Laming, G.; Lee, A. M.; Maslen, P. E.; Murray, C. W.; Rice, J. E.; Simandiras, E. D.; Stone, A. J.; Su, M. D.; Tozer, D. J.

(42) *CRC Handbook of Chemistry and Physics*, 76th ed.; Lide, D. R., Ed.; CRC Press: Boca Raton, FL, 1995.

(43) Krause, H.; H. J. Neusser, H. J. *Chem. Phys. Lett*. **1993**, *213*, 603.

(44) Schauer, M.; Bernstein, E. R. *J. Chem. Phys*. **1985**, *82*, 726

(45) Leutwyler, S. *Chem. Phys. Lett*. **1984**, *107*, 284.

(46) Gotch, A.; Zwier, T. S. *J. Chem. Phys*. **1992**, *96*, 3388.

(47) Carrasquillo, E.; Zwier, T. S.; Levy, D. H. *J. Chem. Phys*. **1985**, *83*, 4990.

(48) Shelley, M. Y.; Dai, H.-L.; Troxler, T. *J. Chem. Phys*. **1999**, *110*, 9081.

(49) Gotch, A. J.; Pribble, R. N.; Ensminger, A.; Zwier, T. S. *Laser Chem*. **1994**, *13*, 187.

(50) Shimanouchi, T. *Tables of Molecular Vibrational Frequencies, Consolidated Volume I*; National Standard Reference Data Series; National Bureau of Standards: Washington, DC, 1972; Vol. 39.

(51) Jeffrey, G. A. *An Introduction to Hydrogen Bonding*; Oxford University Press: Oxford, 1997.

(52) Hobza, P.; Spirko, V.; Selzle, H. L.; Schlag, E. W. *J. Phys. Chem. A* **1998**, *102*, 2501.

(53) Previously reported MP2/6-31G(d) level calculations of the benzene−methane cluster by Hobza et al. (ref 52) show the bond length shortening and small blue shift in the vibrational frequency upon cluster formation. On the other hand, our calculations show the bond length enlargement and small reduction of the C−H stretching frequency. Our calculations agree with the spectroscopic measurements. The observed symmetric C−H stretching frequency is reduced upon cluster formation. The MP2/6-31G(d) level geometry optimization and vibrational analysis by Hobza et al. were carried out without counterpoise correction. The lack of the counterpoise correction should be the cause of the bond length shortening and small blue shift of the C−H stretching frequency. Reimann et al. carried out vibrational analysis of the fluorobenzene−fluoroform cluster using both counterpoise-corrected and not-corrected potential energy surfaces (ref 54). They reported that the MP2/6-31G(d) level calculations without the counterpoise correction underestimate the C−H bond length and overestimate the C−H vibrational frequency compared with the counterpoise-corrected ones. These results show that the effects of counterpoise correction on the calculated geometry and vibrational frequency are not negligible, if the medium-size 6-31G(d) basis set is used for the calculations.

(54) Reimann, B.; Buchhold, K.; Vaupel, S.; Brutschy, B.; Havlas, Z.; Spirko, V.; Hobza, P. *J. Phys. Chem. A* **2001**, *105*, 5560.

(55) Singh, U. C.; Kollman, P. A. *J. Comput. Chem.* **1984**, 5, 129.

(56) Besler, B. H.; Mertz, K. M.; Kollman, P. A. *J. Comput. Chem.* **1990**, *11*, 431.

(57) Herzberg, G. *Molecular Spectra and Molecular Structure*, *Volume II Infrared and Raman Spectra of Polyatomic Molecules*; Krieger Publishing Company: Malabar, 1991.

(58) Pribble, R. N.; Garrett, A. W.; Harber, K.; Zwier, T. S. *J. Chem. Phys*. **1995**, *103*, 531.